Correlation of Chemical Element Properties to Electrochemical Properties of Hydrogen Storage Alloys

Ping Wu* and Kok Liang Heng

Institute of High Performance Computing, 89B Science Park Drive, #01-05/08 The Rutherford, Singapore Science Park I, Singapore 118261

Received October 26, 1998
Revised Manuscript Received January 22, 1999

A fundamental objective of materials research is to understand the mechanism of behavior and to predict the properties of materials. However, it is often difficult if not impossible to study materials, especially alloy hydrides, from the first principle approaches, because of the complex nature of the research. Alternative methods such as correlation techniques must then be developed. Structure mapping[1,2] is one such successful approach. It correlates the crystal structures of materials that have the same chemical stoichiometry but different chemistry to their chemical element properties. Structure maps have, therefore, been widely used to search for materials with specific crystal structures.

The differences in crystal structures are so large that, in a structure map, compounds of different structures are located in distinctively different zones. For compounds having the same crystal structure, they will cluster but not superimpose because differences in chemistry will allow each of them a unique position in the structure map. In our study, all AB_5 alloys have the same crystal structure and are made of the same chemical elements. The traditional structure map techniques are no longer applicable in this case since all alloys will be superimposed to form a point on the structure map. A new approach to the construction of a property map will be developed in this study.

A capacity of an electrode is controlled by a number of factors such as electrode chemistry and surface morphology of the electrode materials.[3−7] Many of these factors could be considered when developing a correlation model. However, the set of factors selected in this study seems to work nicely.

Data regarding AB_5 hydrogen storage electrodes from the literature is listed in Table 1. This table has a total of 44 records, each record has four predictor variables (mole fraction of La, Ce, Nd, and Pr) and two response variables (C_0, charge discharge capacity; S_{200}; capacity retention after 200 cycles). The first 30 records are from Guo et al.,[8] and the remaining 14 records are from Jin.[3]

Table 1. Ni−MH Electrode Data from Guo et al.[8] and Jin[3]

no.	n_{La}	n_{Ce}	n_{Nd}	n_{Pr}	C_0 (mA h/g)	S_{200}
1	0.317	0.135	0.223	0.325	239.4	0.750
2	0.176	0.206	0.124	0.494	240.5	0.520
3	0.528	0.029	0.372	0.071	244.7	0.630
4	0.433	0.040	0.433	0.095	246.4	0.560
5	0.270	0.135	0.270	0.325	233.7	0.760
6	0.150	0.206	0.150	0.494	234.3	0.570
7	0.450	0.029	0.450	0.071	226.9	0.530
8	0.649	0.040	0.216	0.095	244.2	0.630
9	0.405	0.135	0.135	0.325	243.4	0.710
10	0.225	0.206	0.075	0.494	247.2	0.880
11	0.675	0.029	0.225	0.071	248.1	0.860
12	0.288	0.040	0.577	0.095	228.0	0.560
13	0.180	0.135	0.360	0.325	239.8	0.790
14	0.100	0.206	0.200	0.494	228.8	0.560
15	0.300	0.029	0.600	0.071	220.8	0.700
16	0.794	0.066	0.109	0.031	255.6	0.610
17	0.831	0.069	0.078	0.022	270.7	0.600
18	0.277	0.023	0.545	0.155	218.3	0.690
19	0.272	0.272	0.355	0.101	248.2	0.780
20	0.430	0.430	0.109	0.031	258.0	0.560
21	0.450	0.450	0.078	0.022	256.3	0.550
22	0.150	0.150	0.545	0.155	234.1	0.640
23	0.181	0.360	0.355	0.101	233.2	0.680
24	0.287	0.573	0.109	0.031	257.7	0.590
25	0.300	0.600	0.078	0.022	259.2	0.650
26	0.100	0.200	0.545	0.155	225.6	0.760
27	0.518	0.026	0.355	0.101	229.5	0.600
28	0.819	0.041	0.109	0.031	247.8	0.640
29	0.857	0.043	0.078	0.022	259.0	0.660
30	0.286	0.014	0.545	0.155	223.5	0.560
31	0.360	0.450	0.140	0.050	322.0	0.810
32	0.450	0.050	0.390	0.110	318.0	0.750
33	0.400	0.350	0.050	0.200	312.0	0.730
34	0.400	0.200	0.250	0.150	295.0	0.720
35	0.430	0.430	0.050	0.090	326.0	0.760
36	0.590	0.060	0.290	0.060	312.0	0.780
37	0.430	0.300	0.130	0.130	286.0	0.780
38	0.430	0.300	0.150	0.120	317.0	0.790
39	0.740	0.050	0.050	0.160	302.0	0.760
40	0.480	0.240	0.240	0.040	289.0	0.840
41	0.600	0.170	0.140	0.090	296.0	0.780
42	0.600	0.050	0.150	0.200	291.0	0.690
43	0.460	0.270	0.190	0.080	300.0	0.820
44	0.670	0.230	0.050	0.050	311.0	0.800

AB_5 alloys have a hexagonal structure[9] with A atoms (A = La, Ce, Pr, and Nd) occupying sublattice *a* and B atoms (B = Mn, Ni, Co, and Al) occupying sublattice *b* or sublattice *c*. For simplicity, we redefine lattice *a* as lattice 1 and combine lattice *b* and lattice *c* into lattice 2. In AB_5 alloys the nearest neighbor of A atoms are B atoms, and vice versa. The A_i-B_j pairs are the most important interactions in the solid. We applied a two sublattice model for the solid.[10] The lattice fraction is defined as:

* Corresponding author. E-mail: wuping@ihpc.nus.edu.sg. Telephone: (65) 770-9212. Fax: (65) 778-0522

(1) Burdett, J. K.; Rodgers, J. R. *Encyclopedia of Inorganic Chemistry, Volume 7, Rho-S*; King, R. B. Ed.; John Wiley & Sons: New York, 1994; pp 3394−3959.
(2) Villars, P. *Intermetallic compounds Principles and Practice, Volume 1-Principles*; Westbrook J. H., Fleischer R. L., Eds.; John Wiley & Sons: New York, 1995; pp 227−275.
(3) Jin, H. M. Ph.D. Thesis, General Research Institute for Non Ferrous Metals, Beijing, 1997.
(4) Sakai, T.; Hazama, T.; Miyamura, H.; Kuriyama, N.; Kato, A.; Ishikawa, H. *J. Less Common Met.* **1991**, *172*, 1175.
(5) Adzic, G. D.; Johnson, J. R.; Reilly, J. J.; McBreen, J.; Mukerjee, S.; Kumar, M. P. S.; Zhang, W.; Srinivasan S. *J. Electrochem. Soc.* **1995**, *142*, 3429.
(6) Sakai, T.; Meli, F.; Zuttel, A.; Schlapbach, L. *J. Alloys Compds.* **1995**, *221*, 284.
(7) Schlapbach, L.; Seiler, A.; Stucki, F.; Siegmann, H. *J. Less Common Met.* **1980**, *73*, 145.
(8) Guo, J.; Li, C. H.; Liu, H. L.; Chen, N. Y. *J. Electrochem. Soc.* **1997**, *144*, 2276.
(9) Joubert, J.-M.; Cern?, R.; Latroche, M.; Percheron-Guégan, A.; Yvon, K. *J. Alloys Compds.* **1998**, *265*, 311.
(10) Pelton, A. D. Calphad J. **1988**, *12*, 127.

10.1021/cm9810335 CCC: $18.00
Published on Web 04/19/1999

$$Y_{A_i} = \frac{n_{A_i}}{\sum_{i=1}^{4} n_{A_i}} \quad i = 1, ..., 4 \tag{1}$$

$$Y_{B_j} = \frac{n_{Bj}}{\sum_{j=1}^{4} n_{B_j}} \quad j = 1, ..., 4 \tag{2}$$

where n_{A_i} and n_{B_j} are the number of moles of A_i and B_j in lattices 1 and 2, respectively. In this study, the values of n_{Ni}, n_{Co}, n_{Mn}, and n_{Al} were kept constant at 3.55, 0.75, 0.40, and 0.30, respectively.

To build a property map, its coordinates, which will be functions of element properties and element concentrations in the alloy, have to be defined. For an A_i-B_j atomic pair, the difference between atom A_i and atom B_j in terms of element property P (i.e., P_{A_i} for A_i and P_{B_j} for B_j) is

$$Q_{A_iB_j} = |P_{A_i} - P_{B_j}| \tag{3}$$

Subsequently, in a multicomponent and two sublattice alloy, a property map coordinate, O_P (in respect to element property P), was defined as

$$O_P = \sum_{A_i} \sum_{B_j} Y_{A_i} Y_{B_j} Q_{A_iB_j} \tag{4}$$

where $Y_{A_i}Y_{B_j}$ is proportional to the total number of A_i-B_j pairs and O_P is, therefore, the overall element property difference of all nearest neighbor atomic pairs in the alloy.

Some properties of the A_i and B_j elements are listed in Table 2.[11] In the present work, a few element properties such as atomic number (AN), melting point (T), valence electron number (V), and pseudopotential radii (R) were selected to define the property map coordinates based on eqs 1−4. Coordinates O_1, O_2, and O_3 based on element properties AN, T, and V/R^3, respectively, were generated as shown in Table 3 together with C_0 and S_{200}. All records are divided into two classes based on the values of C_0 and S_{200}. Class label C_1 is assigned to be 1 (good class) if $C_0 \geq 250$ and 2 (bad class) if $C_0 < 250$. Similarly, class label C_2 is assigned value 1 (good class) if $S_{200} \geq 0.7$ and 2 (bad class) if $S_{200} < 0.7$.

A simple correlation between the electrochemical properties (C_0 and S_{200}) of AB_5 hydrogen storage alloys and the chemical element properties was established. S_{200} is strongly correlated to T and AN as shown in Figure 1a,b. C_0 is strongly correlated to V/R^3 and AN as in Figure 2a,b.

Figures 1b and 2b may be used in the performance prediction of other elements if applied to replace the elements in AB_5 alloys. As an example, we only replace Nd by Sm, Eu, Gd, Tb, Dy, Ho, Er, Tm, Yb, or Lu, respectively. We select an alloy which may give both high cycle life and high charge discharge capacity: 63% La, 21% Ce, 11% Nd, and 5% Pr.[12] By replacing the 11% Nd by equal moles of Sm, Eu, Gd, Tb, Dy, Ho, Er, Tm, Yb, or Lu, respectively, the model-predicted performance of these 10 alloys are shown in Figures 3 and 4. In Figure 3, new alloys corresponding to Sm, Eu, Er ,and Tm may have high life cycle. In Figure 4, new alloys corresponding to Sm and Eu may have satisfactory charge−discharge capacities. Overall, only Sm and Eu are recommended to replace Nd when the stoichiometry of the alloy is $La_{0.63}Ce_{0.21}X_{0.11}Pr_{0.05}$, X = Nd, Sm, and Eu. New replacement rules may be possible if different chemical stoichiometries are used in the design.

To predict C_0 and S_{200} from the chemical properties, a neural network model was developed for each of the bulk properties. In our case study, a random validation

Table 2. Some Basic Chemical Element Properties[11]

	atomic number	melting temp (K)	valence electron factor	pseudo-pontential radii (Å)
La	57	1193	3	3.080
Ce	58	1071	3	4.500
Nd	60	1283	3	3.990
Pr	59	1204	3	4.480
Ni	28	1726	10	2.180
Co	27	1768	9	2.020
Mn	25	1518	7	2.220
Al	13	933	3	1.675

Table 3. Property Map Coordinates O_1, O_2, and O_3

no.	O_1	O_2	O_3	C_0 (mA h/g)	S_{200}	C_1	C_2
1	31.744	499.966	0.8801	239.4	0.75	2	1
2	31.856	513.793	0.8914	240.5	0.52	2	2
3	31.577	479.243	0.8633	244.7	0.63	2	2
4	31.849	475.867	0.8700	246.4	0.56	2	2
5	31.885	496.243	0.8827	233.7.	0.76	2	1
6	31.934	511.734	0.8928	234.3	0.57	2	2
7	31.811	473.066	0.8676	226.7	0.53	2	2
8	31.168	492.547	0.8570	244.2	0.63	2	2
9	31.480	506.935	0.8752	243.4	0.71	2	1
10	31.709	517.674	0.8886	247.2	0.88	2	1
11	31.136	490.886	0.8550	248.1	0.86	2	1
12	32.251	463.956	0.8772	228.0	0.56	2	2
13	32.155	489.115	0.8878	239.8	0.79	2	1
14	32.084	507.774	0.8956	228.8	0.56	2	2
15	32.261	461.186	0.8760	220.8	0.70	2	2
16	30.745	504.432	0.8483	255.6	0.61	1	2
17	30.637	507.297	0.8462	270.7	0.60	1	2
18	32.258	464.084	0.8784	218.3	0.69	2	2
19	31.829	506.388	0.8814	248.2	0.78	2	1
20	31.109	543.512	0.8738	258.0	0.56	1	2
21	31.018	548.201	0.8728	256.3	0.55	1	2
22	32.385	477.719	0.8873	234.1	0.64	2	2
23	31.920	516.158	0.8878	233.2	0.68	2	2
24	31.252	558.864	0.8838	257.7	0.59	1	2
25	31.168	564.305	0.8833	259.2	0.65	1	2
26	32.435	483.087	0.8908	225.6	0.76	2	1
27	31.583	479.977	0.8642	229.5	0.60	2	2
28	30.720	501.748	0.8466	247.8	0.64	2	2
29	30.611	504.505	0.8443	259.0	0.66	1	2
30	32.249	463.118	0.8778	223.5	0.56	2	2
31	31.260	543.020	0.8783	322.0	0.81	1	1
32	31.730	479.695	0.8685	318.0	0.75	1	1
33	31.190	537.960	0.8767	312.0	0.73	1	1
34	31.540	506.500	0.8739	295.0	0.72	1	1
35	31.050	547.613	0.8746	326.0	0.76	1	1
36	31.340	489.172	0.8601	312.0	0.78	1	1
37	30.937	521.870	0.8645	286.0	0.78	1	1
38	31.280	525.446	0.8732	317.0	0.79	1	1
39	30.810	506.139	0.8529	302.0	0.76	1	1
40	31.330	512.651	0.8685	289.0	0.84	1	1
41	31.060	512.572	0.8615	296.0	0.78	1	1
42	31.190	497.832	0.8613	291.0	0.69	1	2
43	31.290	519.444	0.8706	300.0	0.82	1	1
44	30.770	526.528	0.8578	311.0	0.80	1	1

(11) Samsonov, G. V. *Handbook of the Physiochemical Properties of the Elements*; IFI/Plenum: New York, 1968; pp10−312.

(12) Heng, K. L.; Jin, H. M.; Li, Y.; Wu, P. *J. Mater. Chem*. In press.

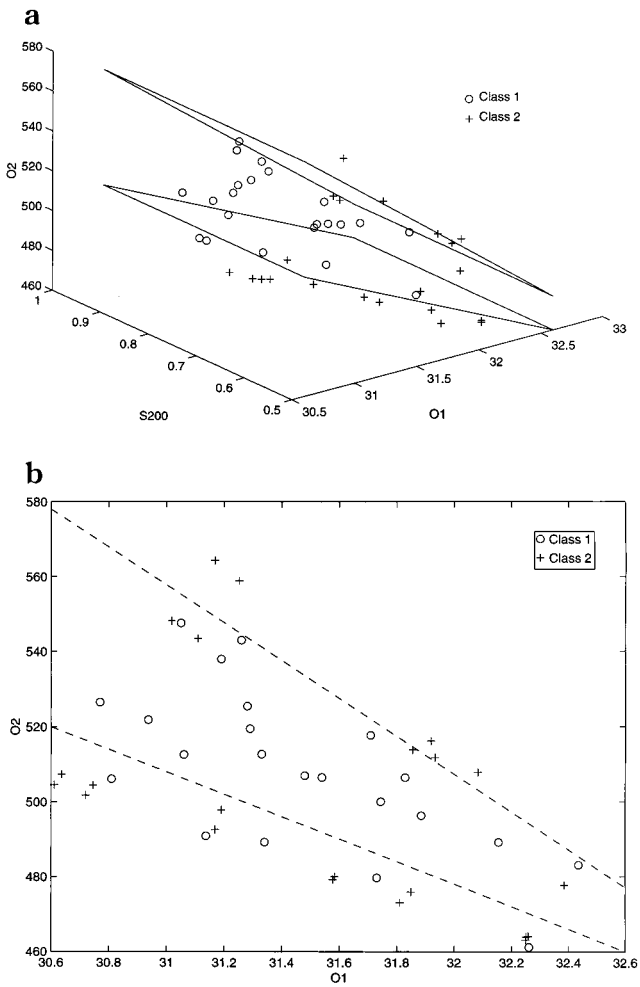

Figure 1. (a) Classification of cycle life using O_1, O_2, and S_{200}. (b) Projection of Figure 1a onto a two-dimensional space (O_1-O_2).

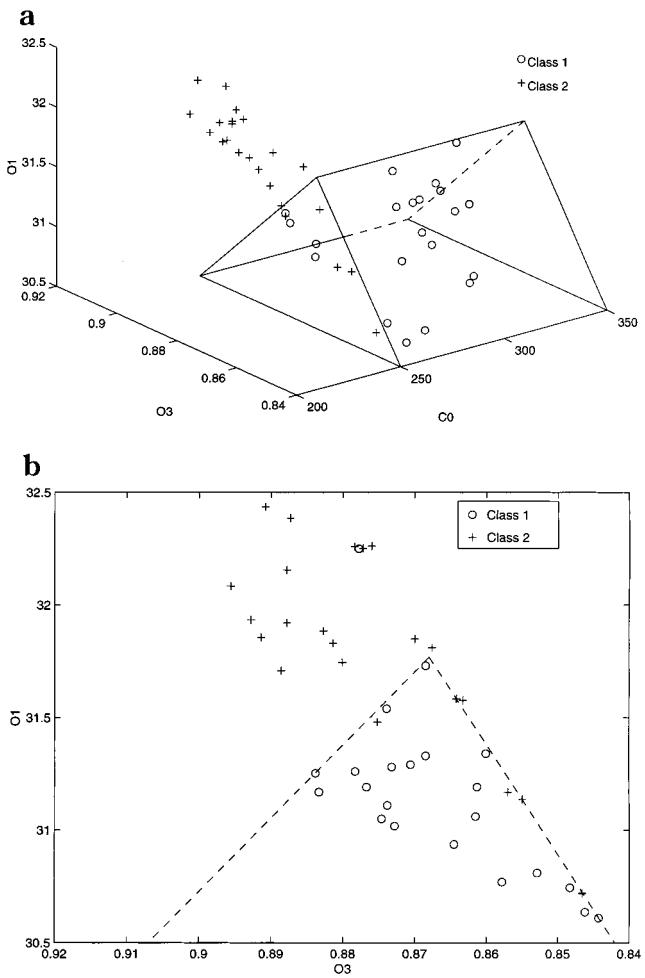

Figure 2. (a) Classification of charge discharge capacity using O_1, O_3, and C_0. (b) Projection of Figure 2a onto a two-dimensional space (O_1-O_3).

set containing 10% of the samples (4 records) was held out to implement early stopping[13] for both the bulk properties. The values of charge−discharge capacity and cycle life from experiments versus those predicted by the neural networks are shown in Figures 5−8. The results of predicted values were in good agreement with the experimental values.

Discussion. In this study, a simple correlation between bulk properties of hydrogen storage alloys and a few properties of their constituent chemical elements was obtained. The correlation may be used in the optimal design of chemistry for hydrogen storage alloys. The correlation may also bring insights to the physics governing S_{200} and C_0.

The melting point and atomic number of the constituent elements were identified to be significant in response to S_{200}. A close relationship between the process of diffusion and melting of metals has been shown by Rice and Nachtrieb.[14] A relation between the activation energy for self-diffusion (Q) and the melting point (T_f) was shown[15]

$$Q = KT_f$$

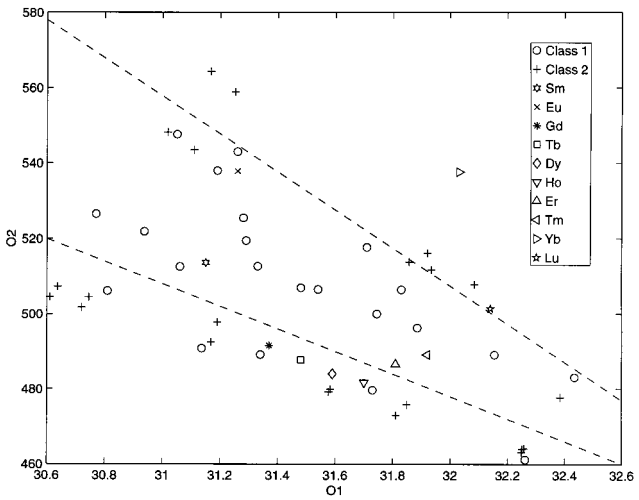

Figure 3. Performance prediction of 10 alloys with respect to cycle life.

where K is a constant and its value is expected to vary from one system to another. Furthermore, Tiwari[16] showed that this correlation between the parameters of self-diffusion and melting is valid for normal metals as well as the metals showing anomalies in their diffusion behavior. Since the element melting point,

(13) Nelson, M. C.; Illingworth, W. T. *A Practical Guide to Neural Nets*; Addison-Wesley: Reading, MA, 1991; p 165.
(14) Rice, S. A.; Nachtrieb, N. H. *J. Chem. Phys.* **1959**, *31*, 139.
(15) Nachtrieb, N. H.; Handler, G. S. *Acta Met.* **1954**, *2*, 797.
(16) Tiwari, G. P. *Z. Metallkd.* **1981**, *72*, 211.

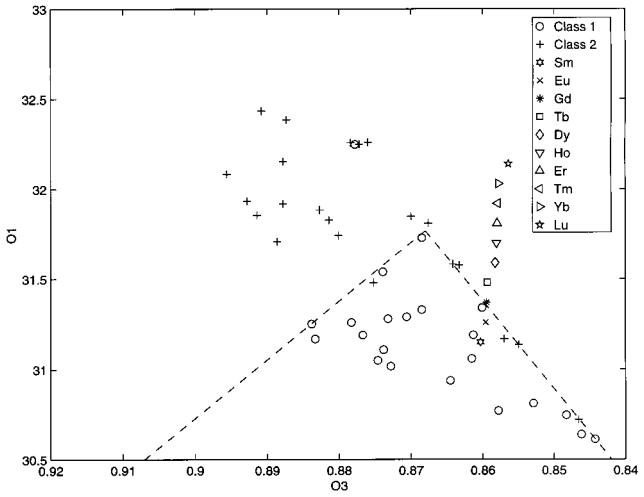

Figure 4. Performance prediction of 10 alloys with respect to charge discharge capacity.

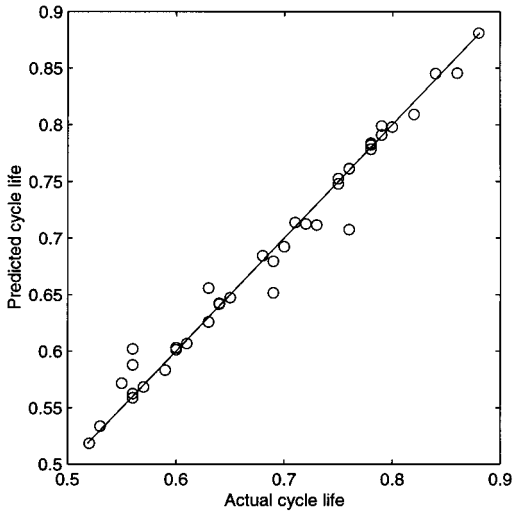

Figure 5. Comparison of actual and predicted cycle life (training set).

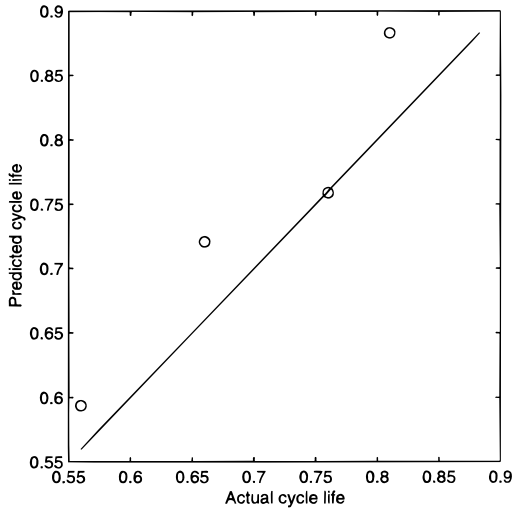

Figure 6. Comparison of actual and predicted cycle life (validation set).

which is strongly related to its self-diffusion parameter, has been identified as one of the most important factors correlating with the value of S_{200}, it may indicate that

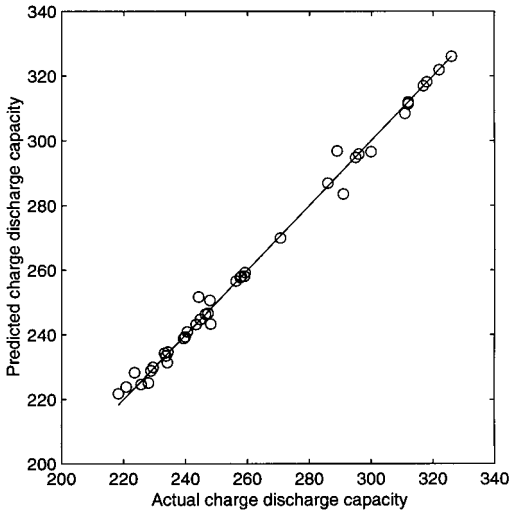

Figure 7. Comparison of actual and predicted charge discharge capacities (training set).

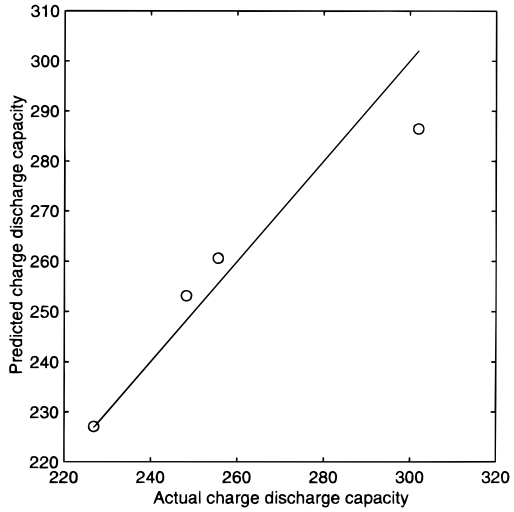

Figure 8. Comparison of actual and predicted charge discharge capacities (validation set).

the diffusion during the sintering process plays an important role in determining the cycle life of the electrodes. A thermodynamic study of these alloys may be useful in order to enhance the sintering process.

The V/R^3 term is proportional to the mean volume valence-electron density. The strong correlation observed between C_0, V/R^3, and AN may suggest that the charge−discharge capacity of electrodes relies on the average valence-electron volume density, which supports the conclusion of Iwakura et al.,[17] who found that charge transfer at the electrodes is responsible for the discharge efficiency.

Acknowledgment. The authors are grateful to Dr. Pierre Villars of MPDS, Switzerland, for fruitful discussions on structure mapping techniques, and to Prof. Steven Bernasek of Princeton University, for helpful comments and suggestions.

CM9810335

(17) Iwakura, C.; Miyamota, M.; Inoue, H.; Matsuoka, M.; Fukumoto, Y. *J. Alloys Compds.* **1997**, *259*, 132.